

Structure of a trimeric domain of the MHC class II-associated chaperonin and targeting protein Ii

Alan Jasanoff^{1,2}, Gerhard Wagner³ and Don C.Wiley^{1,4,5}

¹Department of Molecular and Cellular Biology, ²Committee on Higher Degrees in Biophysics, ³Department of Biological Chemistry and Molecular Pharmacology, Harvard Medical School and ⁴Howard Hughes Medical Institute, Harvard University, Cambridge, MA 02138, USA

⁵Corresponding author

The invariant chain (Ii) plays a critical role in MHC class II antigen processing by stabilizing peptide-free class II $\alpha\beta$ heterodimers in a nonameric ($\alpha\beta$ Ii)₃ complex soon after their synthesis and directing transport of the complex from the endoplasmic reticulum to compartments where peptide loading of class II takes place. Loading progresses following Ii proteolysis and via an intermediate complex of MHC class II with an Ii-derived peptide, CLIP. CLIP is substituted by exogenous peptidic fragments in an exchange reaction catalyzed by HLA-DM. The CLIP region of Ii, roughly residues 81–104, is one of two segments shown to interact with class II HLA-DR molecules. The other segment, Ii 118–216, is C-terminal to CLIP, mediates trimerization of the ectodomain of Ii and interferes with DM/class II binding. Here we report the three-dimensional structure of this trimeric domain, determined by nuclear magnetic resonance (NMR) studies of a 27 kDa trimer of human Ii 118–192. The cylindrical shape of the molecule and the mapping of conserved residues delimit surfaces which may be important for interactions between Ii and class II molecules.

Keywords: immunology/invariant chain/major histocompatibility complex class II/nuclear magnetic resonance/protein structure

Introduction

Because the class II-associated invariant chain peptide (CLIP) segment is absolutely required for the invariant chain (Ii) to promote folding and localization of major histocompatibility complex (MHC) class II heterodimers *in vivo*, deletions including CLIP residues have fatal consequences for Ii performance in antigen processing (Freisewinkel *et al.*, 1993; Bijlmakers *et al.*, 1994; Romagnoli and Germain, 1994). By comparison, deletion of the trimerization ectodomain has a subtler effect, abrogating peptide presentation in some cells (Bertolino *et al.*, 1995) but not the ability of Ii to target and escort class II molecules to endosomes. Deletion of the trimerization ectodomain does eliminate Ii's ability to block class II binding of a DR α -specific antibody, the DR α -binding superantigen TSST-1, and the peptide

exchanger human leukocyte antigen (HLA)-DM, but has no effect on binding of peptides and some DR β -specific ligands (Romagnoli and Germain, 1994; Denzin *et al.*, 1996). These results suggest that an interaction between the Ii domain and the DR α subunit could be involved in regulating DM-assisted CLIP dissociation from class II, as well as in bidentate Ii/class II binding.

Ii is anchored to membranes by a sequence near its N-terminus (Ii 32–56) and contains three domains in its luminal portion (Figure 1A). The first 61 luminal residues, Ii 57–117, have been shown by nuclear magnetic resonance (NMR) and proteolysis experiments to be unfolded and disordered in solution, while comparison of circular dichroism and NMR spectra indicates that most of the next 75 residues, Ii 118–192, form a well-ordered domain (Jasanoff *et al.*, 1995; Park, 1995), but that the last 24 residues, which in the p41 splice variant of Ii follow a 64 residue cathepsin L inhibitor domain (Koch *et al.*, 1987; Bevec *et al.*, 1996), are also disordered (A.Jasanoff, S.Song, A.R.Dinner, G.Wagner and D.C.Wiley, unpublished observations) (Figure 1A). From NMR structural studies, trimeric Ii 118–192 was generated by tryptic digestion of a recombinant form of p31, Ii's 159 residue C-terminal luminal domain (Park, 1995). Chemical cross-linking showed that this segment is trimeric (Park, 1995), and homonuclear TOCSY and ¹⁵N-HSQC spectra indicated that it is symmetric. The three-dimensional structure of Ii 118–192, as determined by NMR, shows that the molecule forms a new trimeric fold geometrically suitable for simultaneous interaction with three MHC class II molecules at a potential class II-binding site suggested by sequence conservation patterns.

Results and discussion

The structure of trimeric Ii 118–192 (27 kDa) was determined using standard multidimensional heteronuclear NMR techniques, with extensive use of partial and complete ²H labeling to enhance the sensitivity of triple-resonance and NOESY spectra. Two methods were used to distinguish inter- from intraprotomer NOEs in the spectra of the trimer. Twenty-three interprotomer H^N-H^C NOEs were identified in the ¹⁵N-NOESY-HSQC spectrum of trimers composed of a mixture of ²H,¹⁵N doubly labeled protomers and unlabeled protomers (Walters *et al.*, 1997) (Figure 1B and C, and Materials and methods). A further 138 definite interprotomer and 494 definite intraprotomer H^C-H^C NOEs were assigned by a new method that took advantage of the ability to create and isolate stable trimers with exactly one ¹³C-labeled protomer and two ²H-labeled protomers: peaks absent from the ¹³C NOESY-HSQC spectrum of these mixed trimers but present in the spectrum of uniformly ¹³C-labeled Ii 118–192 trimers could be assigned as interprotomer NOEs, while peaks present in

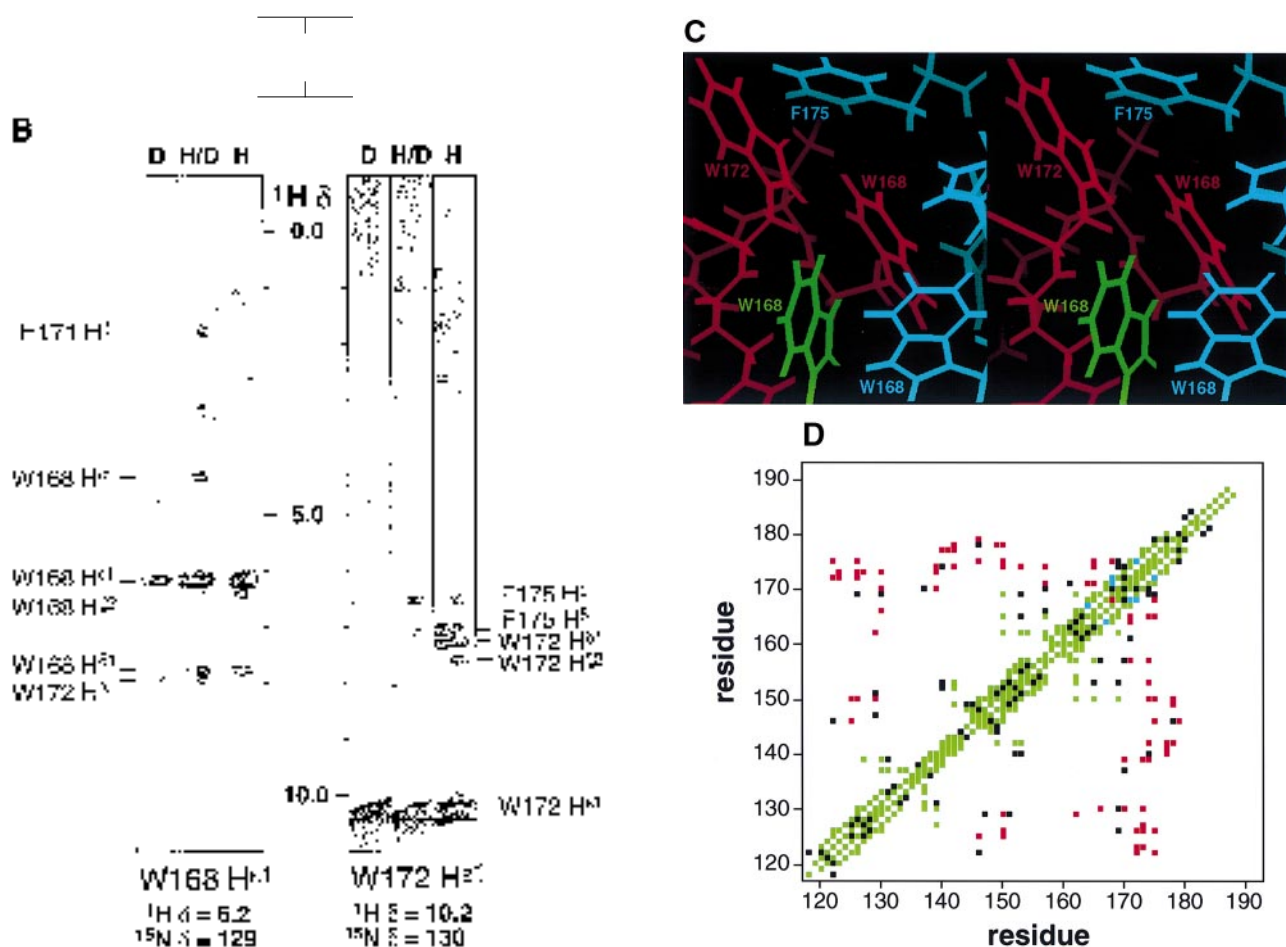


Fig. 1. (A) Organization of the p31 Ii polypeptide. Ii is a type II transmembrane protein. N-terminal residues 1–31 contain a cytoplasmic localization signal, residues 32–56 (TM) span the membrane, and residues 57–216 form the luminal domain. The CLIP region (81–104) is required for efficient Ii-class II complex formation and contains the sequence of a peptide which binds in the class II-binding groove. Residues 118–192 mediate trimerization of the luminal domain and are also involved in class II interactions. (B) Strips of the ^{15}N -NOESY-HSQC spectra of Ii 118–192 showing inter- and intraprotomer NOEs of the W168 and W172 indole protons. Strips from the spectrum of uniformly ^2H , ^{15}N -labeled Ii 118–192 in H_2O (D) show ^{15}NH -NH NOEs only. Strips from the spectrum of mixed trimers containing both ^2H , ^{15}N -labeled protomers and unlabeled protomers (H/D) show ^{15}NH -NH NOEs and interprotomer ^{15}NH -CH NOEs. Strips from the spectrum of non-deuterated ^{15}N -labeled Ii 118–192 (H) show all inter- and intraprotomer NOEs involving ^{15}N -bound protons. (C) Stereoview close-up of the structure of Ii 118–192 showing the proximity of the W168 rings of all three protomers near the 3-fold axis of symmetry and interprotomer contact between W172 and F175, as evidenced by the NOESY spectra of (B). (D) NOE-based interresidue distance restraints used in structural calculations. Green, red and black squares indicate intraprotomer, interprotomer and ambiguous constraints, respectively. Blue squares denote residue pairs for which both inter- and intraprotomer constraints were used.

both spectra could be assigned as intraprotomer NOEs (Jasanoff, 1998). In a trimer, an interprotomer NOE may relate a pair of protons in two protomers either in the clockwise or anticlockwise configuration about the axis of symmetry; determination of the trimeric structure of Ii 118–192 using the resultant ambiguous interprotomer distance constraints may have been facilitated by the number of interprotomer contacts far from the 3-fold axis and between protons far apart in the primary structure (Figure 1D).

The open fold of the Ii 118–192 protomer structure (Figure 2A) is evident in the distribution of (unambiguous) intraprotomer NOEs (green in Figure 1D), which are only found between residues near each other in the sequence and between antiparallel structural elements. Each protomer contains an N-terminal helix A from T122 to A133, connected by an AB strand (134–147) to a second shorter helix B from E148 to T156, a turn, and a longer helix C comprising residues 159–178 (Figure 2A). Helix A makes

no contacts with the B and C helices in the same protomer, but B, C and the BC turn themselves form a compact elbow structure with an angle of 45° and extensive contacts among L150, L153, M157, W162, F165 and M169. The AB strand makes intraprotomer contacts at one end with helix A and at the other end with helix B, and contains four (*trans*) prolines (P135, P140, P141 and P147) which presumably favor its extended structure. The Ii 118–192 fold shows no significant homology to structures in the Protein Data Bank (Holm and Sander, 1995).

Y118 and G119 are partially disordered and show a number of weak NOEs inconsistent with a single conformation. N120 is a glycosylation site (Machamer and Cresswell, 1982), and absence of a polysaccharide in bacterially produced Ii 118–192, in addition to artificiality of the trypsin-generated N-terminus, may influence the conformation of 118–120. C-terminal residues 181–192 are disordered, judging from their narrow linewidths, random coil chemical shifts, and the absence of medium-

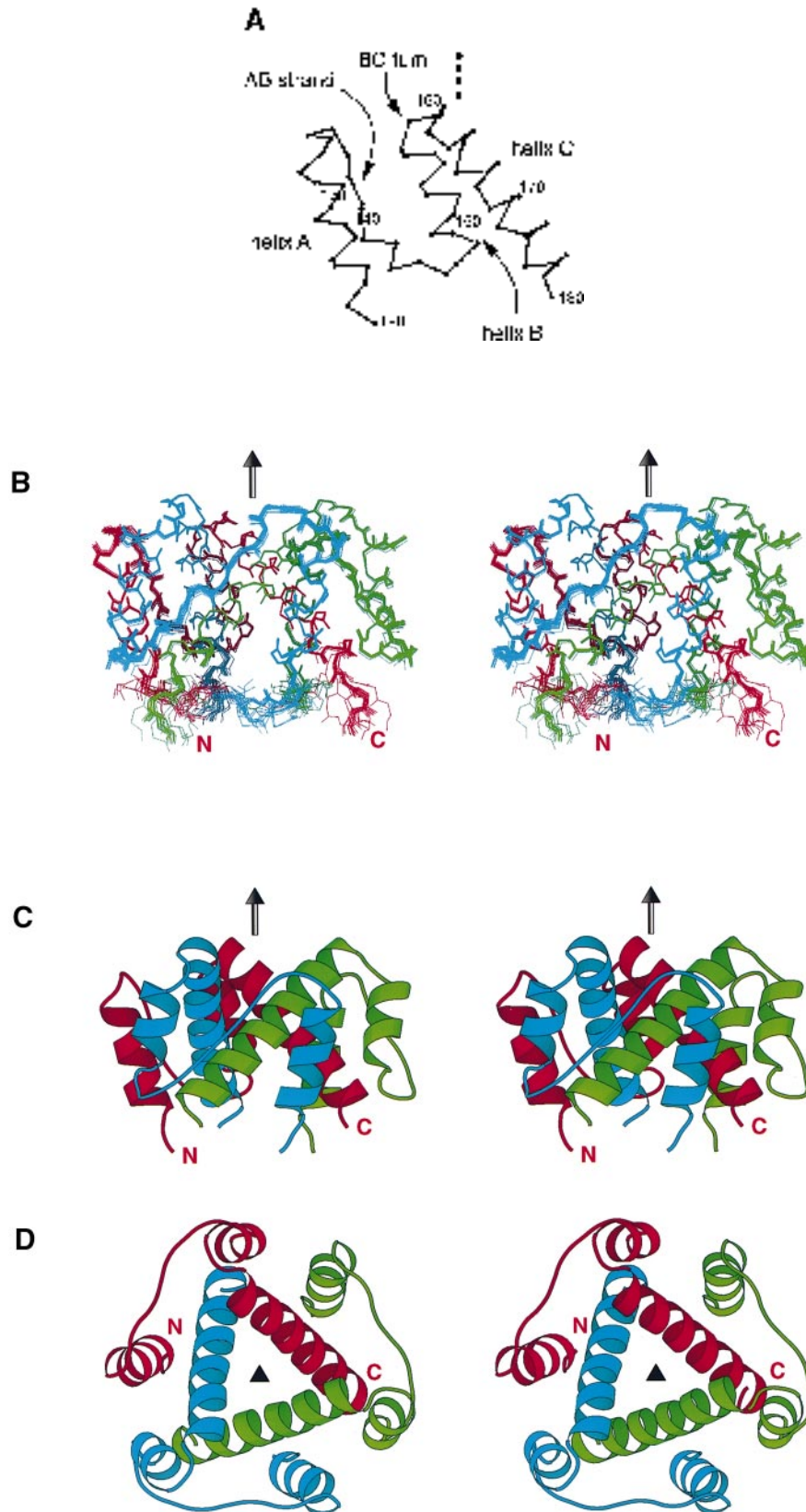


Fig. 2. Structure of Ii 118–192. **(A)** C_{α} trace of a single protomer of Ii 118–192 showing helix A, the AB strand, helix B, the BC turn and helix C. Disordered residues 118–119 and 181–192 are omitted. The gray vertical arrow denotes the axis of 3-fold symmetry. **(B)** Stereoview of a backbone overlay of 20 calculated structures of Ii 118–192 with no NOE-derived distance restraint violations greater than 0.5 Å. The red protomer is in the same orientation as the C_{α} trace of (A), and its N- and C-termini are labeled. Vertical arrows mark the symmetry axis. Residues 118–182 are shown; disorder of 118–119 and 181–182 is apparent. **(C and D)** MOLSCRIPT stereo representations of the minimized average structure of the ensemble in (B) (residues 120–180 shown). Side view **(C)** in the same orientation as in (A) and (B). Top view **(D)** with chain termini pointing away from the viewer. C helices from the three protomers form the core of the structure, with helices A and B surrounding them. Black triangles denote the 3-fold axis, and the termini of the red protomer are labeled.

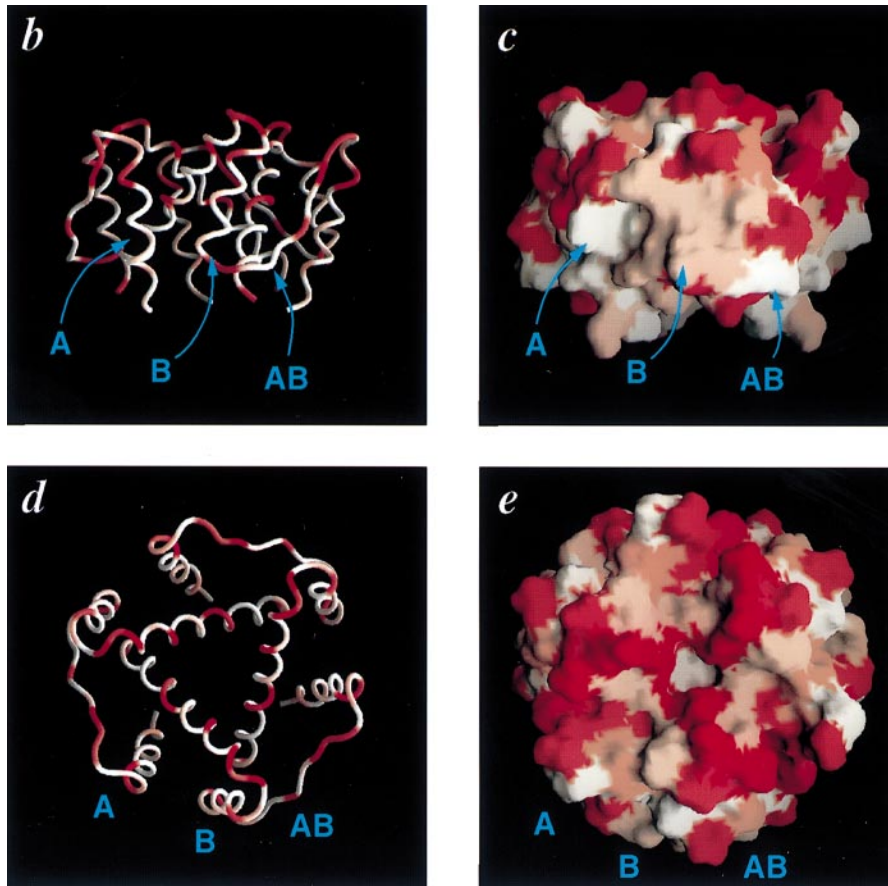
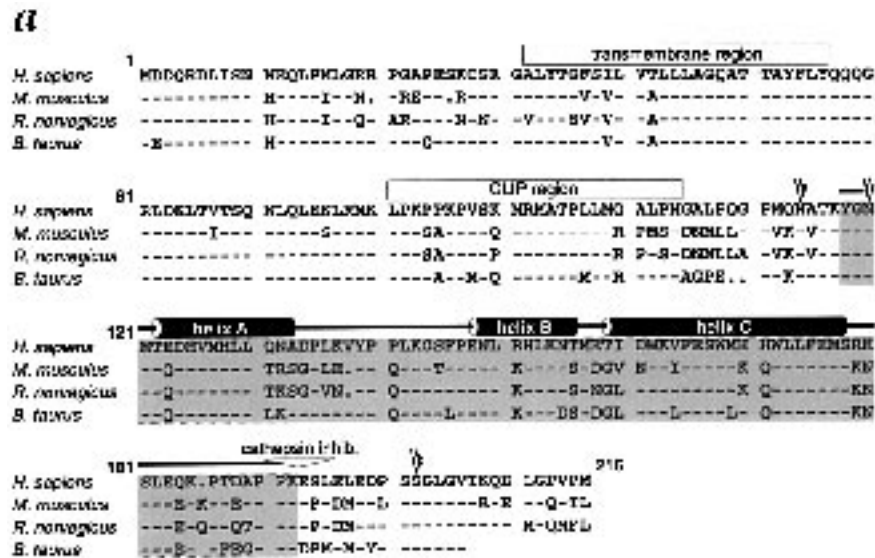


Fig. 3. Sequence conservation in Ii. (a) Comparison of Ii sequences from human, mouse, rat and cow. Residues 118–192 are shaded, and helices A, B, and C are denoted by black tubes. The transmembrane and CLIP regions, and glycosylation sites at N114, N120 and S202 are marked. The p41 form of Ii contains a 64 residue insertion after K192 with cathepsin L inhibition activity and sequence homology to domains from other sources. (b–e) Mapping of sequence conservation to residues in Ii 118–192. A white to red scale correlates with more to less conserved positions. Backbone ‘worm’ (b) and surface (c) representations of a side view of Ii 118–192 showing a patch of conserved residues on the surface, which could correspond to a class II interaction interface and is derived mainly from the A and B helices, and the AB strand of two protomers (blue labels). Backbone ‘worm’ (d) and surface (e) representations of a top view of Ii 118–192. Residues involved in helix–helix packing are well conserved (white), and the most variable surface residues (red) face the viewer. Chain termini are on the opposite face of the molecule.

or long-range NOEs, except for weak signals possibly indicative of transient structure from S181 to Q184. Residues 186, 190 and 191 are prolines, and residues 187–189 and 192 can be shown by NMR to belong to the

disordered C-terminus of a 54 kDa soluble Ii containing residues 72–216. This argues that disorder of C-terminal residues in Ii 118–192 is not an artifact of truncation; their flexibility could be important for accommodating

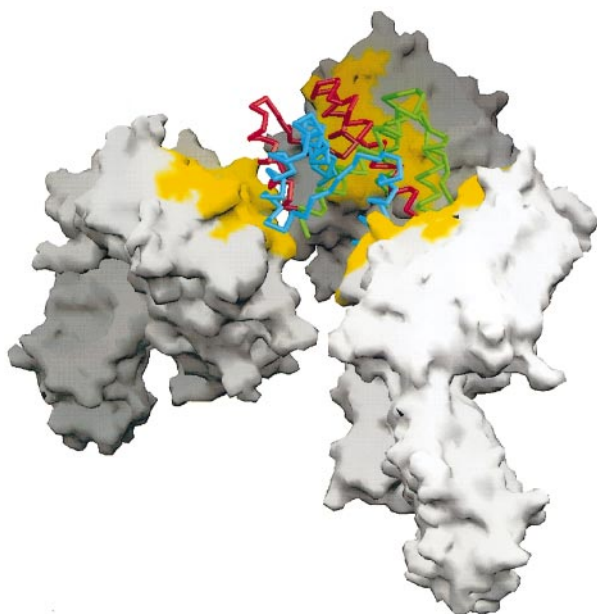


Fig. 4. A hypothetical model of interactions between the Ii 118–192 domain (C_{α} trace) and three MHC class II molecules (surface representation). Ii 118–192 is tilted slightly from its orientation in Figure 2B. In this tentative rendition, the membrane-proximal chain termini of both Ii and class II have been oriented towards the bottom of the page, but Ii 118–192 may rather interact with class II molecules in a configuration with the Ii termini pointing in the opposite direction from the class II termini. Although class II molecules are significantly larger than Ii 118–192, three of them could simultaneously contact the conserved lateral surfaces of the Ii domain without interfering with each other. Yellow patches on the class II molecules, shown here contacting Ii 118–192, correspond to the DR1 α interface with TSST-1 (Kim *et al.*, 1994), a bacterial enterotoxin which competes with Ii for class II binding.

and guaranteeing accessibility of the 64 residue thiol-protease inhibitory domain inserted after K192 in Ii p41 (Koch *et al.*, 1987; Bevec *et al.*, 1996).

The general shape of the Ii 118–192 trimer (Figure 2B–D) is a short cylinder with a diameter of 40 Å and a height of 25 Å, discounting disordered residues. The N- and C-termini emerge, approximately evenly spaced, out of one face of the cylinder. The trimer architecture centers around packing of the C helices, which make extensive interprotomer contacts with each other involving residues 164–175. This explains earlier identification of the 163–183 segment as necessary for Ii trimerization (Bijlmakers *et al.*, 1994; Gedde-Dahl *et al.*, 1997). W168 side chains from the three trimers make edge-to-face contacts at the three C helices' point of closest approach (Figure 1C), resulting in strong interprotomer intraresidue NOEs (Figure 1B) and $^1\text{H}/^2\text{H}$ exchange protection of the indole H^{N} . Considered in pairs, the C helices make angles of $\sim 80^\circ$ against one another, so that the three-helical bundle splays apart at both ends unlike a traditional coiled-coil. The splaying creates pits at both sides of the trimer, lined largely by hydrophilic side chains. Helices A and B form six 'posts' surrounding the core of C helices and almost parallel to the axis of symmetry (Figure 2D).

Ii sequences in the literature are 62% identical over their entire length and 55% identical in the 118–192 region (Figure 3a). Residues which form the hydrophobic core and interprotomer contacts are among those conserved

across all species, including in the chicken Ii sequence (B.Bremnes, M.Rode, M.Gedde-Dahl, S.A.Ness and O.Bakke, submitted) which is only 44% identical to human Ii 118–192. These include T122, V126, L129 and L130 on helix A, Y139 and L142 on the AB strand, L150, L153 and K154 on helix B, and M157 and most of the hydrophobic residues on helix C (Figure 3a). Mapping of sequence variability to the surface of Ii 118–192 shows that the most variable regions are exposed towards the face of the trimer opposite the N- and C-termini (red in Figure 3b–e; top in c). These are at the end of the A helix (131–133), the beginning of the AB strand (134–137) and at the BC turn (156–160). By contrast, more conserved residues (white or light pink in Figure 3b–e) are present on lateral surfaces of the cylinder, closer to the domain's termini, donated primarily by the A helix, the C-terminal half of the AB strand (140–146), and most of the B helix (148–154) (Figure 3c). Although some surface residues (e.g. P140) may be conserved for structural reasons, the asymmetric distribution of variable sites could also reflect evolutionary selection biases at a class II interaction interface.

Due to the relatively small size of the Ii trimerization domain (compared with the class II structure), and the likelihood that Ii and TSST-1 class II-binding sites overlap (Karp *et al.*, 1992; Romagnoli and Germain, 1994), three HLA-DR molecules forming a symmetric complex with Ii 118–192 would probably, for steric reasons, contact lateral sites on the Ii domain. Figure 4 presents a rough but plausible model of such a complex, taking Ii sequence conservation, Ii/enterotoxin class II-binding competition and geometric constraints into account. In intact Ii, the trimerization domain (118–192) is 17 amino acids away from CLIP residues (87–101) which occupy the class II groove in the HLA-DR3–CLIP crystal structure (Ghosh *et al.*, 1995). Our model is therefore consistent with simultaneous interaction of the CLIP region with the class II peptide-binding site and binding of the trimerization domain to the DR α domain in intact ($\alpha\beta$ Ii) $_3$ complexes (Roche *et al.*, 1991).

The structure of Ii 118–192 will facilitate future investigation of Ii's structure–function relationships in the context of antigen presentation *in vivo*. Because of the interdigitation of protomers in the structure, it is unlikely that a single polypeptide of Ii 118–192 could form a stable, ordered structure in the absence of trimeric contacts. Furthermore, mutations which disrupt trimerization of this domain would also disrupt class II interaction interfaces involving more than one protomer. Because of the proximity of the N- and C-termini in Ii 118–192, however, three consecutive end-to-end copies of the 118–192 sequence should be able to form the domain's structure in a single chain Ii. Based on the structure, an engineered single chain Ii containing one copy of the CLIP region could span residues 1–117 followed by three repeats of 118–192 and then the 193–216 sequence, and could be mutated independently at any site, facilitating experiments to distinguish the importance of trimerization and interactions with class II to the function of Ii *in vivo*.

Materials and methods

Ii 118–192 purification and labeling

The soluble invariant chain molecule Ii h94–216, including an N-terminal hexahistidine tag and residues 94–216 of the intact protein, was expressed

Table I. Structural statistics for Ii 118–192

	<i>Interprotomer</i>	<i>Intraprotomer</i>	<i>Ambiguous</i>	<i>All</i>
Number of NOE-derived restraints (total in trimer)				
<i>Intraresidue</i> ($i = j$)	6	186	84	276
Sequential ($ i - j = 1$)	0	690	303	993
Medium ($1 < i - j \leq 4$)	39	663	324	1026
Long ($ i - j > 4$)	339	141	276	756
Total	384	1680	987	3051
R.m.s. restraint violations	0.072 ± 0.004	0.060 ± 0.001	0.091 ± 0.002	0.072 ± 0.001
No. of hydrogen bond restraints in trimer			162	
Average pairwise r.m.s. coordinate differences (residues 120–180):				
Backbone atoms (Å)			0.50	
All heavy atoms (Å)			0.90	
Average r. m. s. deviations from ideal geometry				
Bonds (Å)			0.0058 ± 0.0001	
Angles (°)			0.80 ± 0.01	
Improper angles (°)			0.67 ± 0.01	

in *Escherichia coli* strain XA90 and purified by elution from a nickel column followed by anion exchange chromatography, as described previously (Park *et al.*, 1995). Ii 118–192 was produced by digestion of Ii h94–216 with 50 µg/ml trypsin for ~12 h, followed by quenching with aprotinin or phenylmethylsulfonyl fluoride (PMSF) and anion exchange chromatography (Pharmacia). Isotopic labeling was achieved by growing Ii h94–216-expressing bacteria in 1:1000 inoculated labeled M9 minimal medium cultures at 30°C, with induction at OD₆₀₀ 0.1 by addition of 250 mg/l isopropyl-β-D-thiogalactopyranoside (IPTG). M9 media contained 1.2 g/l ¹³C₆-glucose for production of ¹³C-labeled samples, ¹⁵NH₄Cl for ¹⁵N-labeled samples, and D₂O instead of H₂O for partially (~70%) deuterated samples. Medium for producing 100% perdeuterated samples was also D₂O-based, but contained 1.2 g/l ²H₈-glycerol instead of glucose. Ten per cent ¹³C labeling was accomplished using medium containing 10% ¹³C₆-glucose and 90% ¹²C₆-glucose. Isotopes were purchased from Cambridge Isotope Labs and Aldrich Chemicals. Mixed Ii 118–192 trimers containing ²H,¹⁵N-labeled protomers and unlabeled protomers were produced by mixing labeled and unlabeled protomers in 4 M urea and refolding by dilution. Mixed trimers containing one ¹³C-labeled protomer and two fully ²H-labeled protomers were produced (as described in more detail in Jasanoff, 1998) by mixing ²H-labeled Ii h94–216 with ¹³C-labeled Ii 118–192, purifying mixed trimers with only one ¹³C-labeled protomer by anion exchange, and cleaving with trypsin to generate trimers of Ii 118–192. The efficiency of ²H-labeling was confirmed by NMR, and a non-denaturing polyacrylamide gel-based assay indicated that a non-equilibrium population of mixed Ii 118–192 trimers is stable for many days.

NMR spectroscopy

Spectroscopic data were acquired at 25°C with 0.3–3.0 mM Ii 118–192 in phosphate-buffered saline, pH 6.7, and 0.3 µM aprotinin. The 500 MHz Bruker DMX, Varian VXR and Unity Plus, 600 and 750 MHz Varian Unity INOVA spectrometers were used. Residue-specific backbone assignments were obtained from 500 MHz HNCA and HN(CO)CA spectra of ¹³C,¹⁵N-labeled Ii 118–192, from 500 MHz HNCA, HN(CO)CA, HNCACB and HN(CO)CAB spectra of partially ²H-labeled and ¹³C,¹⁵N-labeled Ii 118–192, and from 100 ms mixing time ¹⁵N-NOESY-HSQC spectra of ¹⁵N-labeled (500 MHz) and ²H,¹⁵N-labeled (750 MHz) samples, all in 93% H₂O/7% D₂O. Side chain resonance assignments were obtained from 50 and 100 ms ¹⁵N-NOESY-HSQC, ¹⁵N-TOCSY-HSQC and HCCH-TOCSY spectra at 500 MHz, and from 50 ms ¹³C-NOESY-HSQC spectra at 750 MHz. Stereospecific assignment of leucine and valine methyl groups was performed using the 600 MHz ¹³C-HSQC spectrum of 10% ¹³C-labeled Ii 118–192. H^N exchange kinetics were determined from ¹⁵N-HSQC spectra following suspension of lyophilized protonated protein in D₂O. Interprotomer-specific H^N-H^C NOEs were recorded from a 750 MHz ¹⁵N-NOESY-HSQC spectrum of the mixed Ii 118–192 trimer containing ²H,¹⁵N-labeled and unlabeled protomers, in 93% H₂O/7% D₂O (Walters *et al.*, 1997). Intraprotomer-specific NOEs were obtained from 750 MHz ¹³C-NOESY-HSQC spectra in 100% D₂O of the Ii 118–192 trimer asymmetrically labeled with ¹³C in one protomer and ²H in the other two protomers (Jasanoff, 1998). NOE-derived distance constraints were

extracted from the 50 ms ¹⁵N-NOESY-HSQC and ¹³C-NOESY-HSQC spectra, and from 100 ms NOESY-HSQC spectra of the ²H,¹⁵N-labeled samples.

Computational methods

Data were processed using Felix (Biosym), and displayed and integrated with XEASY (Xia and Bartels, 1994). Molecular structures were calculated from random starting conformations with 3-fold symmetry by the program X-PLOR, version 3.1 (Brünger, 1992), using a simulated annealing protocol (Nilges, 1993) modified for application to trimers. No dihedral or electrostatic energy terms were used. The following distance restraints were used, per trimer, in addition to symmetry-related constraints: 987 protomer-independent interatomic constraints derived from NOESY spectra of uniformly labeled trimers, 1680 intraprotomer and 384 interprotomer constraints derived from mixed trimer NMR spectra and comparison of similar spectra of mixed and unmixed trimers, and 162 backbone hydrogen bond constraints (1.8–2.5 Å H–O and 2.5–3.3 Å N–O for each NH–O triad), included in later stages of the calculations. Protomer-independent constraints were satisfied if $\sum_{p,q} r_{\text{calc}}^{-6}(p, q)$ was greater than $3r_{\text{cons}}^{-6}$ for each given pair of cross-relaxing protons and all (ordered) pairs of protomers p and q in the trimer, where r_{calc} was calculated from the model and r_{cons} was the constrained distance (Brünger, 1992; Nilges, 1993). Interprotomer constraints were satisfied if $\sum_{p,q} r_{\text{calc}}^{-6}(p, q)$ was greater than $3r_{\text{cons}}^{-6}$ for $p \neq q$, and intraprotomer constraints were satisfied only if $\sum_{p,q} r_{\text{calc}}^{-6}(p, q)$ was greater than $3r_{\text{cons}}^{-6}$ for $p = q$. Of 80 structures calculated by simulated annealing, 35 had no distance violations greater than 0.5 Å, and 25 of these had ϕ and ψ angles only in allowed regions of the Ramachandran plot. Of these 25, four structures with the worst backbone geometry and one with the worst r.m.s. distance constraint violation were eliminated, and the remaining 20 give rise to the figures and statistics we report (Table I). Quanta (Molecular Simulations), GRASP (Nicholls *et al.*, 1991) and Molscrip (Kraulis, 1991) were used for manipulation of atomic models and surfaces.

Acknowledgements

The authors wish to thank Sekhar Talluri, Greg Heffron and Hiroshi Matsuo for technical assistance. Sekhar Talluri, Kylie Walters and Seong-Joon Park are also acknowledged for important discussions and advice. We are indebted to Oddmund Bakke for sharing the sequence of chicken Ii prior to its publication. Funding for purchase of NMR spectrometers from the NIH and HHMI, and additional support from the NIH, NSF, the Harvard Center for Structural Biology and the Giovanni Armenise-Harvard Foundation for Advanced Scientific Research, is gratefully recognized. A.J. was supported by a Howard Hughes Predoctoral Fellowship and D.C.W. is an Investigator of the Howard Hughes Medical Institute. The coordinates of the Ii 118–192 trimer will be deposited in the Protein Data Bank (Upton, NY) and are available from jasanoff@crystal.harvard.edu before release.

References

- Bertolino, P. *et al.* (1995) Deletion of a C-terminal sequence of the class II-associated invariant chain abrogates invariant chain's oligomer formation and class II antigen presentation. *J. Immunol.*, **154**, 5620–5629.
- Bevec, T., Stoka, V., Pungercic, G., Dolenc, I. and Turk, V. (1996) Major histocompatibility complex class II-associated p41 invariant chain fragment is a strong inhibitor of lysosomal cathepsin L. *J. Exp. Med.*, **183**, 1331–1338.
- Bijlmakers, M.J., Benaroch, P. and Ploegh, H.L. (1994) Mapping functional regions in the luminal domain of the class II-associated invariant chain. *J. Exp. Med.*, **180**, 623–629.
- Brünger, A.T. (1992) *X-PLOR (version 3.1) Manual*. Yale University, New Haven, CT.
- Denzin, L.K., Hammond, C. and Cresswell, P. (1996) HLA-DM interactions with intermediates in HLA-DR maturation and a role for HLA-DM in stabilizing empty HLA-DR molecules. *J. Exp. Med.*, **184**, 2153–2165.
- Freisewinkel, I.M., Schenck, K. and Koch, N. (1993) The segment of invariant chain that is critical for association with major histocompatibility complex class II molecules contains the sequence of a peptide eluted from class II polypeptides. *Proc. Natl Acad. Sci. USA*, **90**, 9703–9706.
- Gedde-Dahl, M., Freisewinkel, I., Staschewski, M., Schenck, K., Koch, N. and Bakke, O. (1997) Exon 6 is essential for invariant chain trimerization and induction of large endosomal structures. *J. Biol. Chem.*, **272**, 8281–8287.
- Ghosh, P., Amaya, M., Mellins, E. and Wiley, D.C. (1995) The structure of an intermediate in class II MHC maturation: CLIP bound to HLA-DR3. *Nature*, **378**, 457–462.
- Holm, L. and Sander, C. (1995) Dali: a network tool for protein structure comparison. *Trends Biochem. Sci.*, **20**, 478–480.
- Jasanoff, A. (1998) An asymmetric deuterium labeling strategy to identify interprotomer and intraprotomer NOEs in oligomeric proteins. *J. Biomol. NMR*, **12**, 299–306.
- Jasanoff, A., Park, S.-J. and Wiley, D.C. (1995) Direct observation of disordered regions in the major histocompatibility complex class II-associated invariant chain. *Proc. Natl Acad. Sci. USA*, **92**, 9900–9904.
- Karp, D.R., Jenkins, R.N. and Long, E.O. (1992) Distinct binding sites on HLA-DR for invariant chain and staphylococcal enterotoxins. *Proc. Natl Acad. Sci. USA*, **89**, 9657–9661.
- Kim, J., Urban, R.G., Strominger, J.L. and Wiley, D.C. (1994) Toxic shock syndrome toxin-1 complexed with a class II major histocompatibility molecule HLA-DR1. *Science*, **266**, 1870–1874.
- Koch, N., Lauer, W., Habicht, J. and Dobberstein, B. (1987) Primary structure of the gene for the murine Ia antigen-associated invariant chains (Ii): an alternatively spliced exon encodes a cysteine-rich domain highly homologous to a repetitive sequence of thyroglobulin. *EMBO J.*, **6**, 1677–1683.
- Kraulis, P. (1991) Molscript, a program to produce both detailed and schematic plots of protein structures. *J. Appl. Crystallogr.*, **24**, 946–950.
- Machamer, C.E. and Cresswell, P. (1982) Biosynthesis and glycosylation of the invariant chain associated with HLA-DR antigens. *J. Immunol.*, **129**, 2564–2569.
- Nicholls, A., Sharp, K. and Honig, B. (1991) Protein folding and association: insights from the interfacial and thermodynamic properties of hydrocarbons. *Proteins*, **11**, 281–296.
- Nilges, M. (1993) A calculational strategy for the structure determination of symmetric dimers by ¹H NMR. *Proteins: Struct. Funct. Genet.*, **17**, 297–309.
- Park, S.-J. (1995) *Studies of the Invariant Chain*. Harvard, Cambridge, MA.
- Park, S.-J., Sadegh-Nasseri, S. and Wiley, D.C. (1995) Invariant chain made in *Escherichia coli* has an exposed N-terminal segment that blocks antigen binding to HLA-DR1 and a trimeric C-terminal segment that binds empty HLA-DR1. *Proc. Natl Acad. Sci. USA*, **92**, 11289–11293.
- Roche, P.A., Marks, M.S. and Cresswell, P. (1991) Formation of a nine-subunit complex by HLA class II glycoproteins and the invariant chain. *Nature*, **354**, 392–394.
- Romagnoli, P. and Germain, R.N. (1994) The CLIP region of invariant chain plays a critical role in regulating major histocompatibility complex class II folding, transport and peptide occupancy. *J. Exp. Med.*, **180**, 1107–1113.
- Walters, K.J., Matsuo, H. and Wagner, G. (1997) Use of deuteration to distinguish intermonomer NOEs in homodimeric proteins with C2 symmetry. *J. Am. Chem. Soc.*, **119**, 5958–5959.
- Xia, T. and Bartels, C. (1994) *XEASY User Manual*. ETH-Hönggerberg, Zürich.

Received August 20, 1998; revised and accepted September 25, 1998